

CFD Analysis for the Performance of Gurney Flap on Aerofoil and Vertical Axis Turbine

Yan Yan¹, Eldad Avital², John Williams³

School of Engineering and Materials Science

Queen Mary University of London

327 Mile End Road London E1 4NS UK

Email: yan.yan@qmul.ac.uk¹, e.avital@qmul.ac.uk², j.j.r.williams@qmul.ac.uk³

Theodosios Korakianitis

Parks College of Engineering, Aviation and Technology

Saint Louis University, St Louis, USA

Email: korakianitis@alum.mit.edu

Abstract—A numerical study was carried out to investigate the effects of a Gurney flap on the aerodynamics performance of the NACA 0018 aerofoil and an associated three-blades rotor of a H-type Darrieus wind turbine. The flow fields around a single aerofoil and the Vertical Axis Wind Turbine (VAWT) rotor are studied using URANS. The height of Gurney flap ranges from 1% to 5% of the aerofoil chord length. The flow fields around a single aerofoil and the Vertical Axis Wind Turbine (VAWT) rotor are simulated using URANS. The results show that the Gurney flap can increase the lift and lift-to-drag ratio of the aerofoil. As a result, adding a Gurney flap can significantly improve the power coefficient of the VAWT at low tip speed ratio, where it typically gives low power production. The causing mechanism is discussed in detail

Index Terms—Gurney flap, CFD, wind turbine, aerofoil

I. INTRODUCTION

With the development of industry and economy, the demand for energy has rapidly grown in recent years. Fossil fuel, such as coal and oil, has supported industrial growth in the last century. However, the excessive consumption of fossil fuels has made humanity face an increasing pressure of energy shortage and environment problems, such as global warming and acidic rain. This energy crisis has become a global challenge. The need for alternative environmental friendly energy sources is more acute than ever before

Wind power is one of the most popular renewable energy sources, because of its wide distribution around the globe. A wind turbine can produce electricity by transforming the kinetic energy from wind to the mechanical and electrical energy. Unlike fossil fuels, it produces very little or no greenhouse gas at all, and thus can help efforts in reducing global warming.

Because of the increasing importance of wind energy, improvement in efficiency of wind turbines is of priority, leading to growing research in this area.

There are two types of wind turbines, Horizontal Axis Wind Turbine (HAWT) and Vertical Axis Wind Turbine (VAWT). The former is more popular compared to the latter one, due to its higher aerodynamic power coefficient. However, VAWTs offer some unique advantages that HAWTs do not have. The power production of VAWTs is independent of the incoming direction of the flow. In addition, VAWTs can be deployed to a wide range of wind velocity and produce lower noise. They have relatively simpler mechanical structures and are easier to maintain than HAWTs.

Wind turbine efficiency is mainly determined by the blade shape. The aerofoils are the basic element of the blade. They have significant influence on the aerodynamic performance of the turbine. Nowadays, many methods, such as optimizing blade shape [1, 2], adding intelligent control system and improving the configuration of generator, are available to improve the aerodynamics of wind turbine and overcome the drawbacks. Among them, flow control of wind turbine blades is one of the widely used techniques to improve the power coefficient of the rotor.

The Gurney flap, which is named after its inventor, an American race car driver legend Dan Gurney [3], is a simple but effective passive control device for an aerofoil. Various studies have been carried out to understand the performance of the aerofoil with a Gurney flap and its application on aircrafts and land vehicles. However, its application on the wind turbine blade has not been much investigated.

In the following, the analysis of aerodynamic performance of the Gurney flap on H-type Darrieus wind turbine blade is presented. Detailed flow features around aerofoils is also be discussed.

II. CASE SETUP AND NUMERICAL METHODS

A. Geometry Definition

In this study, unsteady flow computations were carried out for the NACA0018 aerofoil with a Gurney flap. The Gurney Flap is a thin flat tab attached to the trailing edge of an aerofoil on its pressure side. It is normally perpendicular to the chord line[3]. Its length is usually ranging from 0.5% to 5% of the chord. Many wind tunnel tests and numerical studies have been conducted on airfoils with Gurney flaps of different sizes. It was found that this simple device can improve the aerodynamic performance of an airfoil.

Fig. 1 shows the structure of Gurney flap. Its main function is to increase the pressure on the pressure side and decrease the pressure on the suction side of the aerofoil. This results in a higher lift coefficient. This device can also help in delaying separation. Jang et al [4] suggested that the cause was related to the Kutta condition on the airfoil, which means that flow cannot turn around the sharp trailing edge of an aerofoil. The Gurney flap is typically attached perpendicular to the chord line of aerofoil. However, in some cases, a different angle between the flap and the chord can be used.

In the simulation of a single aerofoil, the chord length is 0.246m and the free stream velocity is 10 m/s. The Reynolds number based on the aerofoil chord length is 160K and the Mach number is 0.03, i.e. the flow is incompressible. The C-type structured grid is adopted and the total number of grid points is 70k. There are 200 points along the surface of aerofoil. The radius of the whole computing domain is 30 times of aerofoil chord length.

Gurney flaps of $h=1.0\%$, 2.0% , 3.0% , 4.0% and 5.0% of the chord length were employed. Fig.3 shows the far-field and zoomed view of the computational mesh. No-slip wall boundary condition is implemented on the aerofoil surface. Velocity inlet and pressure outlet boundary condition were used for the computational domain.

In the second part, a study was conducted on a H-type Darrieus wind turbine. The schematic view of this turbine is given in Fig.2. This style of wind turbine has a simple configuration, which is consisting of three vertical blades, one vertical support and six horizontal struts.

The rotor performs in a fixed angular velocity ω . Hence, the blades have a velocity of $R\omega$. The Tip Speed Ratio (TSR) is defined as $\lambda=R\omega/V$ (V stands for the wind velocity). Thus the velocity ‘seen’ by the blade is composed of these two components. Normally the wind turbine is propelled by the force tangential to the struts and the normal force into the struts has no use, except causing stresses.

For this work, a relatively smaller rotor was chosen. To reduce time and resources needed for numerical simulation, a 2D cross-section of H-type turbine was used. This wind turbine is based on the NACA 0018 aerofoil, which can give high lift-to-drag ratio [9]. The main turbine parameters are given in Table I.

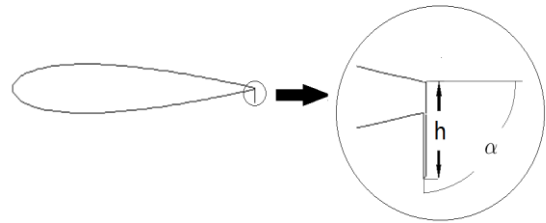


Figure 1. Gurney flap on the aerofoil

TABLE I. ROTOR PARAMETER

Number of blades	3
Blades aerofoil	NACA 0018
Blade chord(L)[m]	0.246
Radius(R)[m]	0.85
Wind speed(V)[m/s]	8
Tip speed ratio	1-3.5

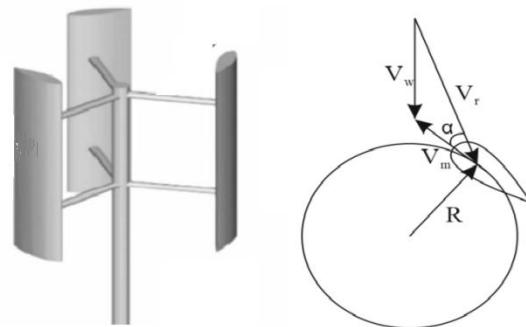


Figure 2. Flow velocity of H-type Darrieus wind turbine

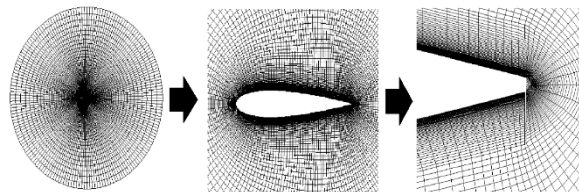


Figure 3. Farfield and zoom view of the computational mesh

The geometry is given in Fig.4. To simulate the rotation of the rotor, the computational domain was divided into two sub-domains (rotor and stator) with an interface between them. The rotor domain is a circular inner zone that includes the actual wind turbine rotor. The wind turbine rotor and the rotor zone have the same rotational angular velocity. The stator domain is a large stationary circular domain outside the inner zone. The mesh on both sides of the interface have the same cell size to achieve a smooth and sliding transition between the two.

The turbine was assumed to operate in an open field. To avoid wall blockage, the computing domain should be large enough. In this work, the radius of stator domain is 10 times of radius of turbine. The radius of rotor zone is 1.5 times of the turbine.

The inlet boundary was set as velocity inlet boundary with a constant wind speed of 8 m/s and the outlet was set as pressure outlet with atmosphere pressure value. The turbine operated with a fixed wind speed and the rotation speed of turbine changed, to achieve different tip speed ratios.

Structured mesh was chosen for the whole domain to reduce the computational time. Fig.5 shows that the dimensionless wall distance (y plus) of the first point away from the blades surface was less than 3. This indicates that mesh in the boundary layer was well resolved.

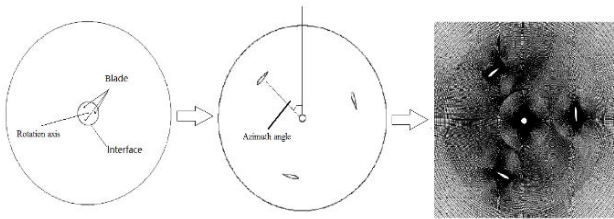


Figure 4. Geometry and mesh of H-type Darrieus wind turbine.

B. Numerical Methods

In this study, ANSYS Fluent was used to generate the 2D CFD model. A finite volume method was applied. The solver was set as pressure based in the unsteady RANS version. Spatial and temporal second order accuracy was used. The SIMPLE approach was used for the time marching and scheme convergence was observed per time step.

The SST (Shear Stress Transport) $k-\omega$ turbulence model was chosen in this work as it has shown good performance in turbo-machinery experiencing flow separation[5] as expected for the blades of VAWT during part of the rotation. The time step was set as 0.001 second, leading to about 670 time steps for one cycle of rotation when the tip speed ratio (TSR) was one. For a larger TSR, a lower time step was chosen to keep about the same number of time steps per cycle.

The simulation was run until a periodic behavior was achieved. If the instantaneous torque coefficient of turbine was less than 1% different than the value on the same azimuth angle of last period, the simulation was considered to be converged. Typically, this happened after around 10 revolutions. The phase averaged values of the following 5 revolutions after the convergence were used as the final result.

III. RESULTS AND DISCUSSIONS

A. Isolated Aerofoil

Figs. 6 & 7 show a comparison of the lift and drag coefficients between our numerical and available experimental results in the literature [6]. As can be seen, the numerical results agree well with the measurements. The “clean” data is from the aerofoil without a Gurney flap, whereas the lines denoted as ‘GFx%’ are the cases where the aerofoils are equipped with Gurney flaps. The length of the Gurney flaps is ‘x%’ the aerofoil chord

length. In Fig.6, the time averaged lift coefficient (C_l) increases as the Angle of Attack (AoA) rises. However, the stall angle decreases from 14° of the clean aerofoil case to 12° of the case with a 5% Gurney flap. The lift coefficient at AoA= 0° also increases significantly and it reaches 0.5 for the 5% Gurney flap case.

Fig. 7 shows the time-averaged drag coefficient for the same configuration. Obviously, as the angle of attack increases, the drag coefficient increases as well. It is also clear that the aerofoil with a larger Gurney flap has a higher drag coefficient.

Fig. 8 presents the pressure coefficient distribution around the aerofoil with and without Gurney flap at AoA= 5° . It can be seen that the Gurney flap can effectively increase the loading on the aerofoil. With the increasing height of the Gurney flap, the pressure difference between the lower and the upper surface of aerofoil becomes larger, especially near the trailing edge where the Gurney flap is attached. This is consistent with the change of the lift coefficient versus angle of attack given in Fig.6.

Fig. 9 shows the pressure coefficient at AoA= 13° . Compared to the smaller angle of attack at 5° , the loading increases due to the presence of the Gurney flap including near the leading edge of aerofoil. When the height of the Gurney flap is larger than 2% chord length, the loading could not be improved anymore with a further increase of the Gurney flap height.

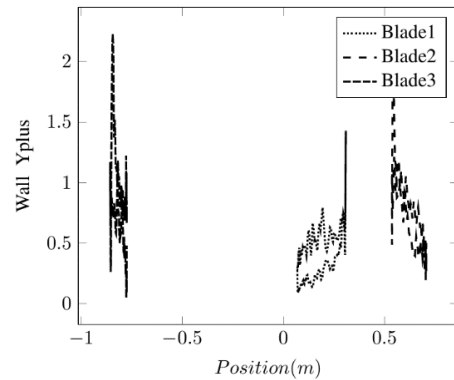


Figure 5. Yplus value for all blades

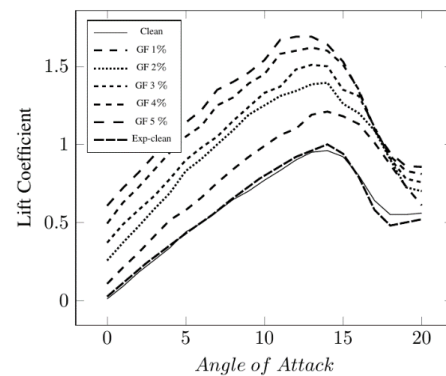


Figure 6. Lift coefficient of aerofoil[6]

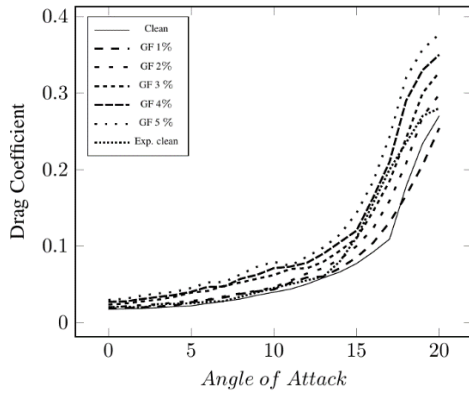


Figure 7. Drag coefficient of aerofoil[6]

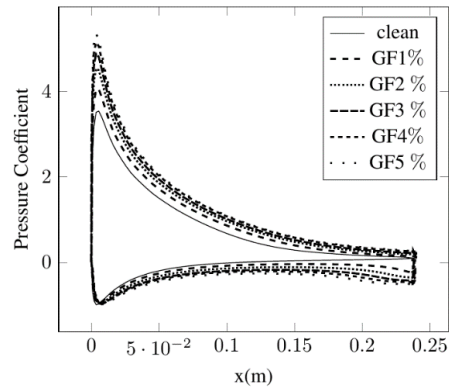


Figure 9. Pressure coefficient on the aerofoil at AoA=13°

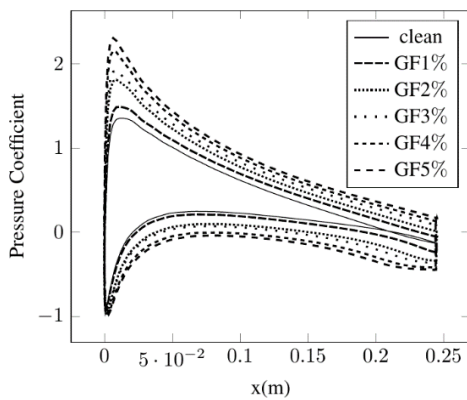


Figure 8. Pressure coefficient on the aerofoil at AoA=5°

Fig. 10 gives the variation of the separation point on the suction side of aerofoil with different Gurney flap lengths. It is clear that the Gurney flap changes the flow separation significantly. The Gurney flap delays the onset of separation point.

At AoA=5°, compared to the clean aerofoil, the 1% chord Gurney flap moves the separation point downstream by 2%. This value can reach 5%, if the height of Gurney flap increases to 2% chord length. At AoA=10° the effect of Gurney flap on the separation point is much stronger. A Gurney flap of 2% chord length moves the separation point downstream by 18%. However, it should be noted that the separation point does not change for the Gurney flap length larger than 2%.

To understand the influence of Gurney flap on the aerofoil performance better, Figs. 11 to 13 compare the streamlines of flow field with and without Gurney flap. At AoA=0° in Fig.12, there is no separation near the trailing edge of the clean aerofoil. However, two separation regions form, one downstream of the Gurney flap, and the other upstream of the Gurney flap on the pressure surface. Due to the presence of the Gurney flap, the pressure on the pressure surface increases, and thus the lift increases as well. In addition, there are two strong vortices at the downstream of the Gurney flap. These vortices reduce the adverse pressure gradient near the trailing edge, which delays the separation on suction side. For all the reasons above, the Gurney flap is an effective and efficient device for the lift enhancement.

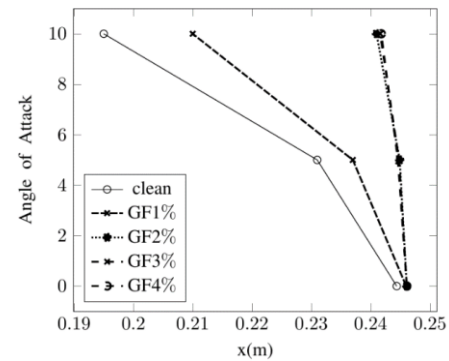


Figure 10. Separation point variation versus angle of attack of different aerofoils

Fig.12 predicts time-averaged velocity distribution near wake region at AoA=9°. It is obvious that a separation bubble appears near the upper surface on the trailing edge of clean aerofoil because of the adverse pressure gradient, which reduces the suction pressure significantly. However there is no noticeable separation bubble on the suction side if the Gurney flap is added. A similar result was found by T. Yu [10]. This phenomenon agrees well with the calculated separation locations given above.

Fig.13 presents the effect of the size of the Gurney flap on flow separation. The separation bubble on the suction side for aerofoil marked with GF3% is much stronger than that of GF5%, which can give an explanation why the lift force increased with the increasing of size of Gurney flap.

A numerical simulation was also conducted to investigate the effect of the angle between the Gurney flap and chord line on the aerodynamic performance of the aerofoil. In this work the Gurney flap with a size of 1% chord length was chosen for discussion. As shown in Fig.14, “GF1%_X” refers to the angle between the Gurney flap and chord line of aerofoil as “X”. It can be seen that the Gurney flap perpendicular to the chord has better performance for improving lift force compared to other two angles near the stall condition by around 5%. On the other hand, the angle of Gurney flap has relatively small influence on the drag force as seen from Fig.15.

B. The VAWT

The verification of the computational framework of VAWTs was conducted by comparing to the published results. Fig.16 shows the comparison of measured data and CFD results in terms of power coefficient versus tip

speed ratio. The rotor's characteristics in current study is the same as in the publication (experiment and CFD work by [9]).

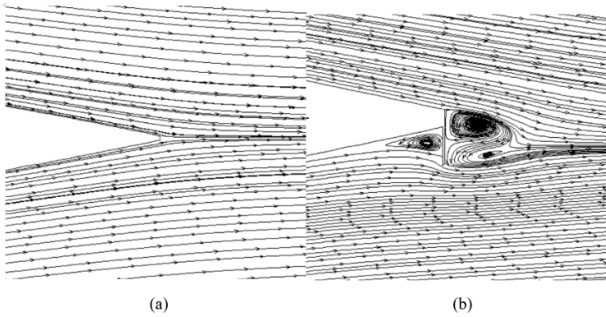


Figure 11. The streamlines in vicinity of aerofoils at $AoA=0^\circ$ (a) Clean aerofoil (b) GF3%

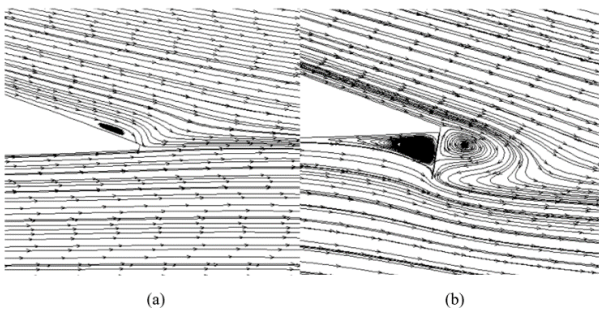


Figure 12. The streamlines in vicinity of aerofoils at $AoA=9^\circ$ (a) Clean aerofoil (b) GF3%

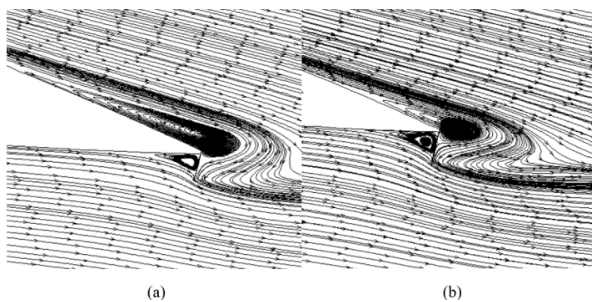


Figure 13. The streamlines in vicinity of aerofoils at $AoA=13^\circ$ (a) Clean aerofoil (b) GF3%

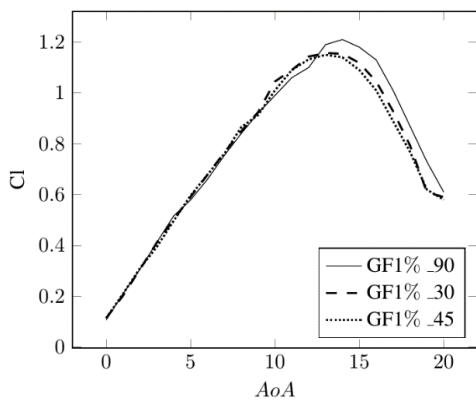


Figure 14. Lift coefficient of aerofoil

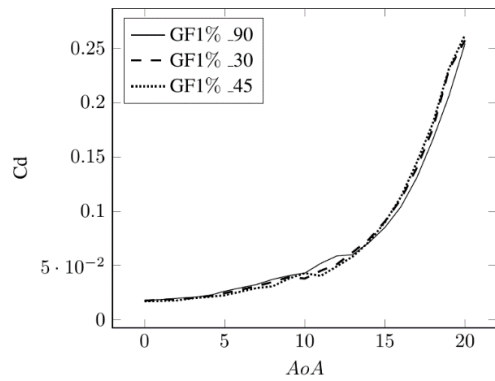


Figure 15. Drag coefficient of aerofoil

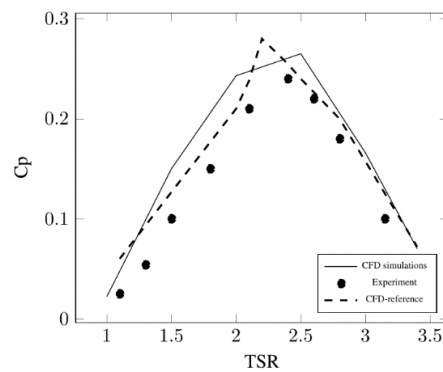


Figure 16. Comparison of power coefficient of VAWTs of experiment and CFD results [9].

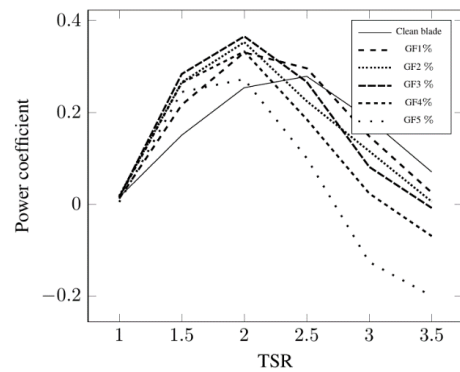


Figure 17. Comparison of power coefficient of VAWTs with and without Gurney flap

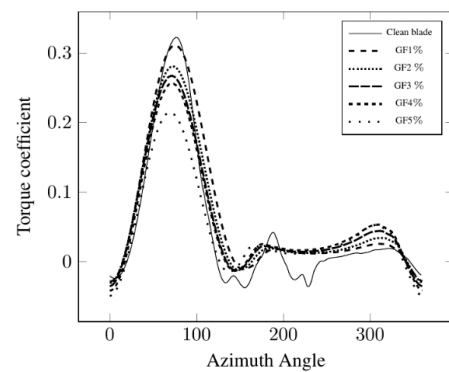


Figure 18. Torque coefficient VAWTs versus azimuth angle for different VAWTs, $TSR=2$

It is obvious that our simulation results agree well with the CFD results of F. Balduzzi [9]. This good match is partly due to the fact that in the experiment a very long blade was chosen to reduce the influence of the tip-loss [9]. This result demonstrates that the present CFD procedure is suitable for predicting the aerodynamic performance of this rotor model.

The performance of a wind turbine is determined by several factors. The shape of aerofoil is a crucial element among them [1]. The VAWT performs at TSRs from 1 to 3.5, where the power output from turbine is of practical interest.

Fig. 17 shows the power coefficient variation at different TSRs. Gurney flaps with different lengths have been installed on the trailing edge of aerofoils. The clean aerofoil case is also superimposed for comparison. From the figure, it can be seen that adding the Gurney flap increases the power coefficient at lower TSRs (from 1 to 2.5). However, as TSR goes above 2.5, the Gurney flap reduces the power coefficient.

The power coefficient does not change too much with different lengths of Gurney flap at TSR=1. However, as the TSR increases to 2, a noticeable variation of power coefficient can be observed from different Gurney flaps. It is interesting that the peak performance of clean blade is at TSR=2.5. However, when a Gurney flap is installed, the power coefficient peaks at TSR=2. It also should be noted that there is an optimal length of Gurney flap which gives maximum power coefficient at TSR=2. For current study, the optimal length of Gurney flap is 2% chord length. When the height of the Gurney flap is larger than 2% chord length, the power coefficient starts to decrease.

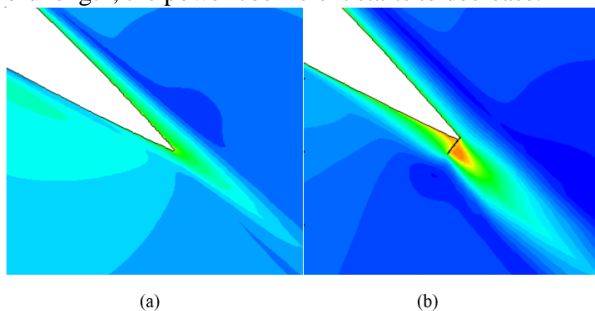


Figure 19. Instantaneous velocity contour at azimuth angle=310 Torque coefficient versus azimuth angle for different VAWTs (a) Clean aerofoil (b) GF3%

Fig.18 shows the torque coefficient versus azimuth angle in one revolution for one blade with and without Gurney flap, at TSR=2. As seen in the figure, the first half of the revolution, the turbine with clean aerofoil has higher power output than that with a Gurney flap. However, during the second half revolution when the blade is at the rear, the blade with a Gurney flap performs better. This means that the tangential force on the blade was increased. The benefit of Gurney flap at the second half of the revolution is larger compared to the reduction at the first part. This can be further explored by exploring the flow field around the blade. Fig.19 illustrates the flow field near trailing edge of turbine blade. It shows the instantaneous velocity contour at azimuth angle=310 ° and TSR=2. It is clear that there is a vortex downstream of the

Gurney flap, where the flow velocity is relatively high. As a result, the pressure difference between the leading edge and trailing edge is larger than in the clean blade, which leads to a large tangential force on the turbine blade.

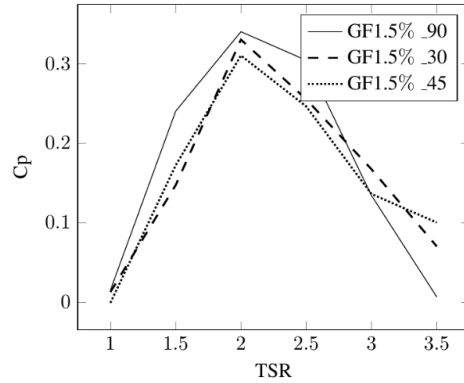


Figure 20. Comparison of power coefficient of VAWTs with different Gurney flap

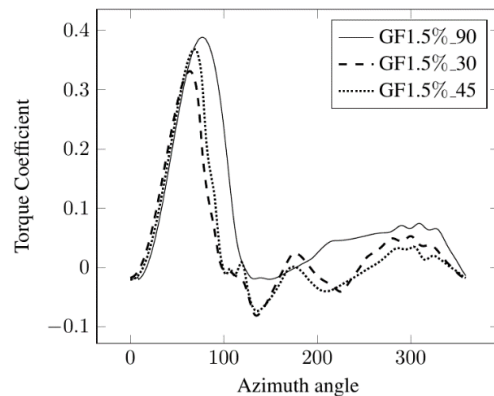


Figure 21. Torque coefficient versus azimuth angle for different VAWTs, TSR=1.5

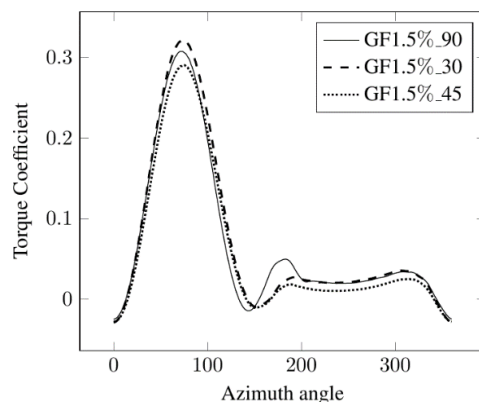


Figure 22. Torque coefficient versus azimuth angle for different VAWTs, TSR=2

Fig. 20 shows how the installation angle of Gurney flap affects the aerodynamic performance of the wind turbine. The Gurney flap of 1.5% chord length was investigated. As we can see in the figure, the Gurney flap perpendicular to the chord of aerofoil performs best

compared to other angles. This finding agrees well with the result of single aerofoil.

The torque coefficient versus azimuth angle at different TSR are present in Fig.21-23. At TSR=1.5 and 2.5, the turbine with Gurney flap of an installation angle of 90 perform s better with a larger torque coefficient at the first half of rotation. The similar conclusion could be drawn from Fig.24 and Fig.25, which show the flow field near turbine blade. It is clear that the pressure difference between the leading edge and trailing edge is larger when the installation angle of Gurney flap is 90.

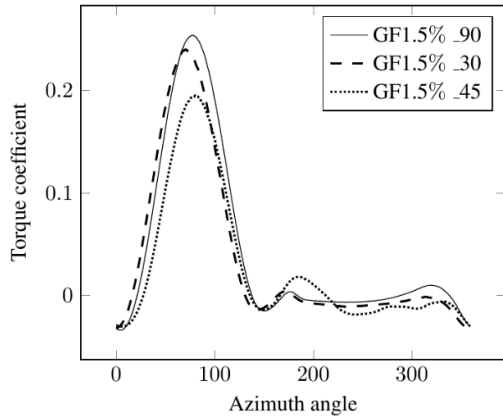


Figure 23. Torque coefficient versus azimuth angle for different VAWTs, TSR=2.5

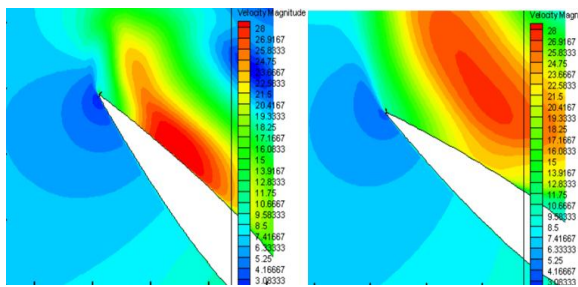


Figure 24. Instantaneous velocity contour at azimuth angle 120 Torque coefficient versus azimuth angle for different VAWTs (a)GF1.5%_90 (b) GF1.5%_45

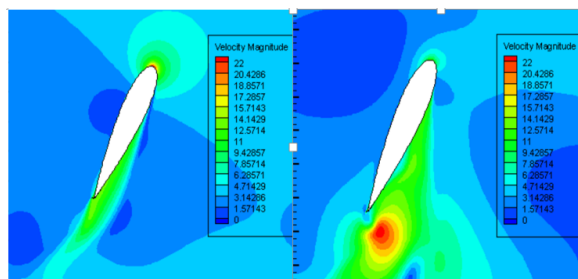


Figure 25. Instantaneous velocity contour at azimuth angle=240 Torque coefficient versus azimuth angle for different VAWTs (a) GF1.5%_90 (b) GF1.5%_45

IV. CONCLUSIONS

Numerical simulation was performed on the two dimensional aerofoil NACA 0018 and H-type Darrieus wind turbine to examine the aerodynamic performance of adding a Gurney flap. Good agreement between the CFD

results and available experimental results were observed both for a single aerofoil and a small scale Darrieus wind turbine.

The results showed that both lift coefficient and lift-to-drag ratio could be increased when a Gurney flap was installed on the trailing edge of the aerofoil. This enhancement become even greater when the height of Gurney flap increased. However. There is an optimal high, beyond which, the performance starts to decrease. The results also showed that the Gurney flap perpendicular to the chord line of aerofoil had the best effect compared to other installation angles. Adding a Gurney flap yielded an increase in the power coefficient for low tip speed ratios from 1 to 2.5.

ACKNOWLEDGMENT

The support of the China CSC scholarship and Queen Mary University of London is kindly acknowledged

REFERENCES

- [1] X. Shen, E. Avital, G. Paul, M. A. Rezaenia, P. Wen, T. Korakianitis, "Experimental study of surface curvature effects on aerodynamic performance of a low Reynolds number airfoil for use in small wind turbines," *J Renewable Sustainable Energy*, vol. 8, no. 5, pp. 053303, 2016
- [2] Y. Yan, E. J. Avital, X. Shen, J. Gao, X. Li, T. Korakiantis, "Aerodynamic and aeroacoustic redesign of low speed blade profile," *ICSV 24*, London, 2017.
- [3] C. Van Dam, D. Yen, and P. HW Vijgen, "Gurney flap experiments on airfoil and wings," *Journal of Aircraft*, vol. 36, no. 2, pp. 484-486, 1999.
- [4] J. Wang, Y. Li, and K.-S. Choi, "Gurney flap lift enhancement, mechanisms and applications," *Progress in Aerospace Sciences*, vol. 44, no. 1, pp. 22-47, 2008.
- [5] F. Menter, "Zonal two equation kw turbulence models for aerodynamic flows," in *23rd fluid dynamics, plasma dynamics, and lasers conference*, 1993, pp. 2906.
- [6] R. E. Sheldahl and P. C. Klimas, Aerodynamic characteristics of seven symmetrical airfoil sections through 180-degree angle of attack for use in aerodynamic analysis of vertical axis wind turbines. Technical report, Sandia National Labs., Albuquerque, NM (USA), 1981.
- [7] D. Troolin, E. Longmire, and W. Lai, "Time resolved piv analysis of flow over a naca 0015 airfoil with gurney flap," *Experiments in Fluids*, vol. 41, no. 2, pp. 241-254, 2006.
- [8] M. Mohamed, A. Ali, and A. Hafiz, "CFD analysis for h-rotor darrieus turbine as a low speed wind energy converter. Engineering Science and Technology," *Engineering Science and Technology, an International Journal*, vol. 18, no. 1, pp.1-13, 2015.
- [9] F. Balduzzi, A. Bianchini, R. Maleci, G. Ferrara, and L. Ferrari, "Critical issues in the CFD simulation of darrieus wind turbines," *Renewable Energy*, vol. 85, pp. 419-435, 2016.
- [10] T. Yu, J. Wang, and P. Zhang, "Numerical simulation of gurney flap on rae-2822 supercritical airfoil," *Journal of Aircraft*, vol. 48, no. 5, pp. 1565-1575, 2011.



Yan Yan received her BSc and MSc degree in Mechanical Engineering from Xi'an Jiaotong University, in 2012 and 2015 respectively. She is currently a PhD student in the school of engineering and material science, Queen Mary university of London. Her areas of interest are computational fluid dynamics, fluid Mechanics and acoustics, wind and water turbines.



Eldad Avital is currently a reader in the school of engineering and material science, Queen Mary university of London. He is the fellow of the Royal Aeronautical Society, fellow of the UK Higher Education Academy, senior member AIAA and member in EuroMech. Dr. Avital's current research interests include: Fluid Mechanics and Acoustics: Computational Aero-Acoustics,

Aerodynamics and Hydrodynamics, Fluids-Structure Interaction, Bio-Fluids.



Theodosios Alexander (aka T. Korakianitis) is the Director of interdisciplinary research collaborations at Saint Louis University. The UK National Health Service Innovations Program awarded Alexander with the Innovator of the Year Award in 2008 and 2009 for his personal research on mechanical circulatory support devices and actively pursues the development and

commercialization of these devices in St. Louis. Alexander's research career has focused on thermal/fluid sciences and applications on the design of power and propulsion systems, energy conversion systems, renewable energy and engineering systems and components. He also conducts research on unsteady thermo-fluid dynamics and unsteady transport phenomena within those areas, the performance of turbomachinery and airfoils, a novel method to predict gas turbine and piston engine emissions, development of a novel Nutating disc engine for unmanned aerial vehicles and on fluid-dynamic modeling of the cardiovascular system, and development of mechanical circulatory support devices.



Prof John Williams is currently a Emeritus Prof of Computational Fluid Dynamics at Queen Mary university of London. His current research interests include Computational fluid dynamics of environmental flows, Large Eddy and Direct Numerical Simulation of free-surface flows, modelling of flow in compound channels, over rough beds and submarine fins.